Geophysical Research Letters

RESEARCH LETTER
10.1029/2022GL102677

Energy Surplus and an Atmosphere-Land-Surface "Tug of War" Control Future Evapotranspiration

Donghui Xu[1,2], Valeriy Y. Ivanov[2], Elizabeth Agee[2,3], and Jingfeng Wang[4]

[1]Atmospheric Sciences and Global Change Division, Pacific Northwest National Laboratory, Richland, WA, USA, [2]Department of Civil and Environmental Engineering, University of Michigan-Ann Arbor, Ann Arbor, MI, USA, [3]Environmental Sciences Division, Oak Ridge National Laboratory, Oak Ridge, TN, USA, [4]Department of Civil and Environmental Engineering, Georgia Institute of Technology, Atlanta, GA, USA

Key Points:

- Maximum Entropy Projection theory yields robust estimates of evapotranspiration (ET) under a warmer climate
- Available energy surplus and supply-demand interactions result in temporally linear increase of ET over the contiguous U.S
- ET and precipitation changes result in uneven spatial distribution of water availability (precipitation minus ET)

Supporting Information:

Supporting Information may be found in the online version of this article.

Correspondence to:

D. Xu and V. Y. Ivanov,
donghui.xu@pnnl.gov;
ivanov@umich.edu

Citation:

Xu, D., Ivanov, V. Y., Agee, E., & Wang, J. (2023). Energy surplus and an atmosphere-land-surface "tug of war" control future evapotranspiration. *Geophysical Research Letters*, *50*, e2022GL102677. https://doi.org/10.1029/2022GL102677

Received 4 JAN 2023
Accepted 18 JUN 2023

Author Contributions:

Conceptualization: Donghui Xu, Valeriy Y. Ivanov
Data curation: Donghui Xu
Formal analysis: Donghui Xu
Funding acquisition: Valeriy Y. Ivanov
Investigation: Donghui Xu, Valeriy Y. Ivanov, Elizabeth Agee, Jingfeng Wang
Methodology: Donghui Xu, Valeriy Y. Ivanov, Elizabeth Agee, Jingfeng Wang
Project Administration: Valeriy Y. Ivanov
Resources: Donghui Xu
Software: Donghui Xu, Elizabeth Agee, Jingfeng Wang

Abstract The 21st century evapotranspiration (ET) trends over the continental U.S. are assessed using innovative, energy-based principles. Annual ET is projected to increase with high confidence at the rate of 20 mm for every 1°C of rise in near-surface air temperature, or 0.45 or 0.98 mm/year/year, depending on the emission scenario. The ET trajectory is dominated (58%) by the increase of land-surface net radiative energy. An enhancement of the fraction of energy taken up by ET becomes a more important controller (53%) in late 21st century, under the high emission scenario. This increase is explained by the "tug of war" between atmospheric vapor demand and land-surface ability to supply water. An assessment of future water availability (precipitation minus ET) shows no significant changes at the continental scale. This outcome nevertheless hides strong spatial variability, emphasizing the role of ET in shaping the distribution of water availability among human populations.

Plain Language Summary Water quantity in the environment is strongly controlled by its evaporation into the atmosphere from plants, soil, and water bodies—the process that is called evapotranspiration. This study calculates evapotranspiration trend over the U.S. during the 21st century and assesses factors determining its evolution. Annual evapotranspiration is predicted to grow at the rate of 20 mm for every 1° Celsius of rise in near-surface air temperature, leading to 14%–23% increase with respect to the historic period, depending on climate scenario. This increase is due to the impacts of future greenhouse gas emissions on energy that fuels evapotranspiration, as well as interplay between the growing water vapor demand by the atmosphere and changing land-surface water supply conditions in the warmer climate. The predicted evapotranspiration trends will result in the strengthening of uneven distribution of water quantity across the U.S. in the future.

1. Introduction

Evapotranspiration (ET) represents a critical terrestrial process (Fisher et al., 2017), involving considerable amounts of water (Good et al., 2015; Oki & Kanae, 2006) and energy (Trenberth et al., 2009) at global scales. Therefore, ET has significant impacts on large-scale processes of the climate system and water resource availability, as well as smaller-scale conditions of environmental and human habitat quality. Future changes in land-surface ET may impact water availability with important environmental and societal implications. Robust estimates of surface water and energy flux partitioning are needed to project ET trends to further understand land-atmosphere feedbacks (Seneviratne et al., 2010) to the ongoing climate change.

ET is difficult to measure and estimate at large spatial scales. Previous studies have thus identified historic ET trends of conflicting signs and magnitudes. Satellite-based data and model outputs (Mao et al., 2015; Yao et al., 2016; Zeng et al., 2012; Zhang et al., 2015, 2016) depict a positive trend of global ET over the past decades, attributing it to an increase in surface net radiation (Wild et al., 2008), warmer air temperatures, and vegetation "greening" (Zhang et al., 2015; Zhu et al., 2016). Other studies argue in favor of a recent global ET decline (Xiao et al., 2020). Various process proxies have been scrutinized to explain the perceived decline in ET. Soil moisture controls constraining regional ET (Jung et al., 2010), internal climate variability (Miralles et al., 2014), or vegetation responses (Xiao et al., 2020) have been cited as the likely reasons.

The net effect of vegetation physiological processes is particularly elusive. High air vapor pressure deficit (VPD) corresponds to high potential ET but may cause plants to close leaf stomata (Oren et al., 1999) with the resultant

Supervision: Valeriy Y. Ivanov, Jingfeng Wang
Validation: Donghui Xu, Elizabeth Agee
Visualization: Donghui Xu
Writing – original draft: Donghui Xu
Writing – review & editing: Donghui Xu, Valeriy Y. Ivanov, Elizabeth Agee, Jingfeng Wang

decrease of canopy conductance to vapor flux and the suppression of total ET (Xiao et al., 2020). Whether the projected increase in VPD will reach a threshold triggering the conductance decline is a point of active discussion (Grossiord et al., 2020). Further, drier soils can additionally limit plant water supply. As future conditions are projected to be drier (Dai, 2013) and with globally higher VPD (Wei et al., 2012; Yuan et al., 2019), the relative roles of VPD, canopy conductance, and soil moisture in modulating the land-surface responses to the changing climate has been debated (Humphrey et al., 2021; Liu et al., 2020; Novick et al., 2016; Sulman et al., 2016). Plant physiological responses to rising CO_2 and changes in canopy biomass have been cited to exert significant effects on ET (Lemordant et al., 2018; Milly & Dunne, 2016; Swann et al., 2016), or, conversely, their net effects have been deemed neglible (Tor-ngern et al., 2015).

Previous studies have used outputs of Earth System Models (ESMs) to understand the ET response to climate change (Ajjur & Al-Ghamdi, 2021; Berg & Sheffield, 2019; Lu et al., 2021; Sullivan et al., 2019), generally projecting positive ET trends in the future. However, ESM ET simulations show substantial biases (e.g., Sullivan et al., 2019), likely stemming from the use of variables and surface conductance parameterizations of high uncertainty. ET biases reinforce low confidence in ESM projections and their limited ability to infer relevant driver attributions (Text S1 in Supporting Information S1). Another approach to the problem is warranted. Maximum Entropy Production (MEP) theory (Wang & Bras, 2009) is a parsimonious, energy-based principles formulation rooted in thermodynamics that can constrain the uncertainties of ET projections. MEP model formulates energy dissipation partitioning of land-surface net radiative energy into latent, sensible, and ground heat fluxes. The model requires fewer inputs than classical ET algorithms, avoiding typical parameterization uncertainties (Text S2 in Supporting Information S1), and it has demonstrated a well-proven accuracy for a variety of land-cover conditions (Huang et al., 2017; Isabelle et al., 2021; Nearing et al., 2012; Shanafield et al., 2015; Sun et al., 2022; Wang et al., 2014; Xu et al., 2019), offering the potential to elucidate mechanisms controlling future ET changes.

In this study, we use the MEP-based method to analyze how terrestrial ET will change over the contiguous United States (CONUS) during the 21st century, driven by the latest set of projected climate trajectories. The MEP-based ET estimates are first demonstrated to have a high skill during the historical period as compared to a regional product of high accuracy (Livneh et al., 2013). ESM radiative energy and hydrometeorological outputs are further used as inputs to MEP to project ET under different CO_2 emission scenarios. Regions exhibiting high "signal-to-noise" ratio in ET projections (Knutti & Sedláček, 2012) are identified and discussed. The projected ET changes of high confidence permit a subsequent attribution analysis with respect to the primary controlling factors. The projected spatiotemporal distribution of ET and precipitation prompt the analysis of future water availability across CONUS. Overall, this research shows how climate change-induced energy, atmospheric vapor demand, and land-surface conditions will control the future ET and water availability.

2. Materials and Methods

2.1. Climate Model Projections

Seventeen ESMs that contributed to the Coupled Model Intercomparison Project Phase 6 (CMIP6; Eyring et al., 2016) were selected in this study (Table S1 in Supporting Information S1) based on their availability of monthly net radiation (Rn), near-surface air temperature (T_s), specific humidity (q_s), top layer soil moisture (θ), latent heat flux (λE), and precipitation (Pr). The emission scenarios of the Shared Socioeconomic Pathways (SSP; O'Neill et al., 2017) 2–4.5 and 5–8.5 are used here to represent medium and the "business-as-usual" cases of the projected CO_2 emissions. Three time periods are chosen for the analysis: control period (1961–1990), mid-century (2041–2070), and end-century (2071–2100). ET simulated with the MEP model using ESM-generated inputs is referred to as "MEP-based ET." ET provided in ESM outputs is referred to as "ESM-based ET."

2.2. Maximum Entropy Production Model

A brief description of the MEP model is in Text S2 in Supporting Information S1 and readers are referred to Wang and Bras (2009, 2011) for a detailed formulation, and Hajji et al. (2018) for its enhancement to be suitable for applications in water stress conditions. MEP model validation shows a significantly improved skill of simulating ET during the historical period as compared to the ESM-based ET estimates (Text S3 in Supporting Information S1). Additionally, a sensitivity analysis suggests the parameter values used in MEP are appropriate for their use in ET projections (Text S3 in Supporting Information S1). Note that the MEP theory does not explicitly

account for plant physiological responses to higher CO_2 (e.g., changes in canopy conductance) and changes in vegetation structure (e.g., expansion or decrease of leaf area). These short- and long-term scale responses are implicitly accounted for through the corresponding changes in the MEP model inputs: net radiation and near-surface temperature and humidity, which are obtained from ESMs (Section 2.1).

2.3. Surface Conductance

Generally, latent heat flux (λE; the energy flux associated with ET process) can be estimated as a function of VPD and surface conductance (g_c) (Sellers et al., 1997):

$$\lambda E = \frac{\rho c_P}{\gamma} \mathrm{VPD}\, g_c, \tag{1}$$

where ρ is the air density, c_P is the air heat capacity, and γ is the psychrometric constant. Given the MEP-estimated flux λE and ESM-simulated VPD, one can inversely estimate g_c from Equation 1. This permits the attribution of λE increase in the future due to the changes in Rn and its partition, as presented in Texts S5 and S6 in Supporting Information S1.

2.4. Water Availability

The net water flux into the surface from the atmosphere, that is, precipitation minus evapotranspiration over land (Konapala & Mishra, 2020), is another variable of particular interest. It is commonly used as an indicator of water availability (WA) at both short-term and long-term (climate) scales:

$$\mathrm{WA} = Pr - \mathrm{ET}, \tag{2}$$

3. Results

3.1. ET Spatial Change in the Future

MEP-based estimates project an increase of ET over the CONUS under different CO_2 emission scenarios (Figure 1). Specifically, MEP model projects higher increase of ET in the Eastern US and Pacific regions than in the rest of CONUS. The ET changes are mainly attributed to the increase of transpiration component of ET (Figure S6 in Supporting Information S1). According to the robustness metric (RM, see details in Test S7) of Knutti and Sedláček (2012), the MEP-based projections exhibit strong agreement (RM > 0.8) among the selected models over 52.7%, 60%, 65.1%, and 81.7% of the CONUS for the SSP245 mid-century, SSP245 end-century, SSP585 mid-century, and SSP585 end-century scenarios (cells with the white and red stipples in Figure 1). The change of ET under the SSP585 scenario has the highest degree of robustness at the end-century, suggesting the larger the consistency of MEP-based ET estimates for larger projected greenhouse gas concentrations. The higher CO_2 concentration intensifies ET process in the MEP-based projections since R_n, temperature, and VPD will be higher. It is remarkable that robustness of the primary MEP model input—R_n—is lower than that of estimated ET (not shown). ESM-based ET projections (Text S7 in Supporting Information S1) show different patterns of ET change. However, these estimates exhibit low robustness due to the high multi-model ensemble uncertainty. The rest of the analysis is hence based on the MEP-based ET estimates.

3.2. Change of ET at Continental Scale and Attributions

ET trend over CONUS (Figure 2a) is larger for SSP585 than for SSP245 scenario, with comparable multi-model ensemble uncertainties (i.e., ∼22% of the ensemble mean). The MEP method projects an increase of CONUS-averaged annual ET at a nearly constant rate of 0.45 [mm/year/year] for SSP245 and 0.98 [mm/year/year] for SSP585, as inferred from the multi-model ensemble means. The increase of projected MEP-based ET is proportional to the increase of temperature (Figure S10a in Supporting Information S1), at the rate of 20 mm/yr for every 1°C increase in near-surface air temperature. Consequently, by the end of century, CONUS-averaged ET is projected to increase by 14% and 23% relative to the control period of 1961–1990 for SSP245 and SSP585 scenarios, respectively.

The increased temperature is not the direct cause for the increase of ET in the future. When one considers the MEP model as a prognostic tool with flux and state inputs (i.e., Rn,T_s,q_s,θ, see Text S2 in Supporting Information S1),

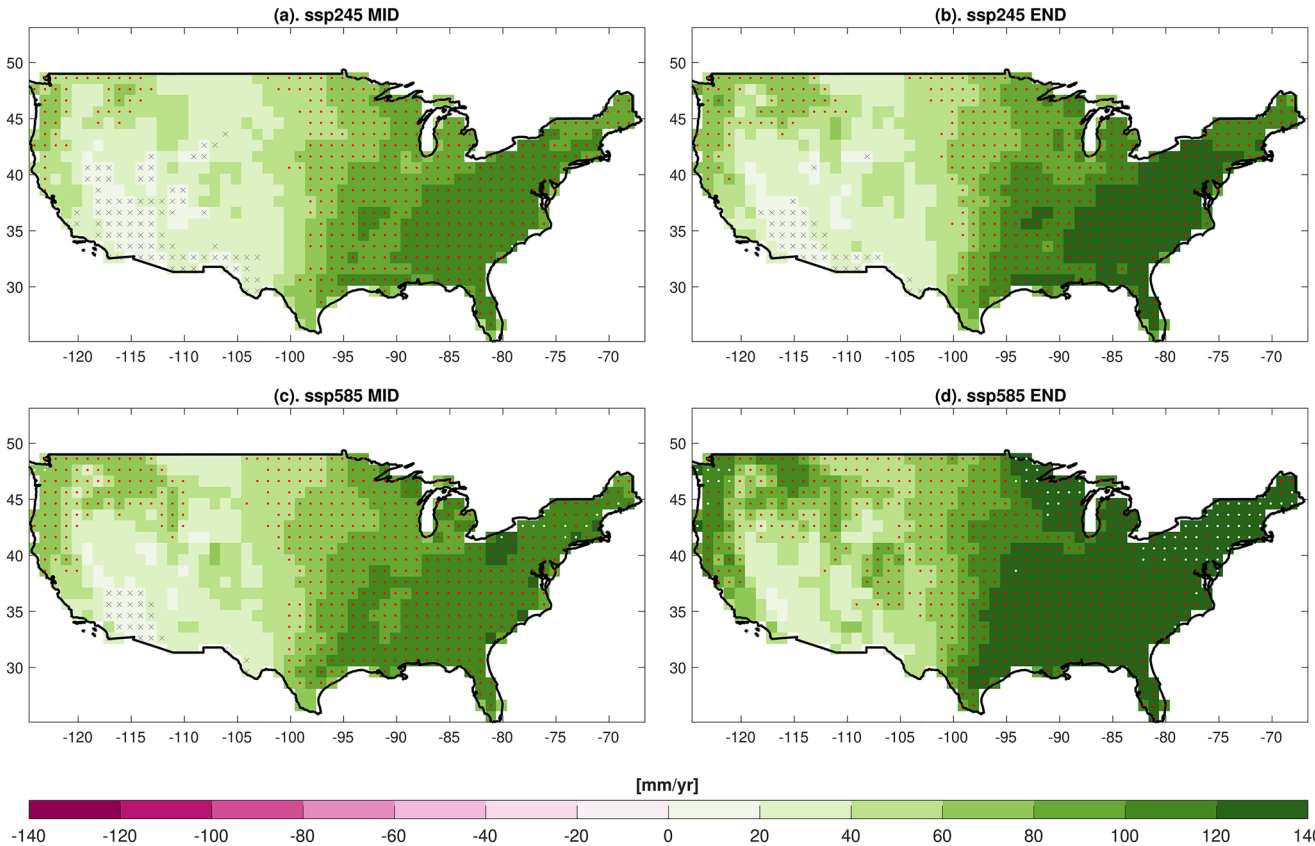

Figure 1. Change of the mean annual ET based on MEP model estimates between the control (CTL) and future periods (FUT). The difference (FUT–CTL) is estimated as the mean of the equal-weighted multi-model ensemble. The grid cells corresponding to good ($0.8 < RM < 0.95$) and high robustness ($RM > 0.95$) of the projection are stippled with red points and white dots, respectively. The grid cells with the cross sign imply low robustness of the projection inference ($RM < 0.5$). "MID" represents the difference between 2041–2070 and 1961–1990 periods, and "END" represents the difference between 2071–2100 and 1961–1990 periods. All of the results are shown at a $1° \times 1°$ resolution.

Rn has been identified as the most sensitive input variable (Isabelle et al., 2021; Xu et al., 2019). The strong correlation between ET and temperature in Figure S10a in Supporting Information S1 stems from the fact that the increase of near-surface temperature is proportional to the increase in Rn: the two are related through a physical theory and results confirm their strong inter-relationship (Figure S11 in Supporting Information S1). Not only an increase in Rn can lead to larger ET in future, but also changes in the partition of available radiative energy into heat fluxes. Consistent with this reasoning, Figure 2c illustrates an increase in the ratio of latent heat flux to net radiation($^{\lambda E}/_{Rn}$, termed hereafter *evaporative allocation of net available energy*), indicating that hydrometeorological factors also contribute to the future ET temporal increase across CONUS (Figures 1 and 2a).

Specifically, in its simplest form (Equation 1), λE (used interchangeably with ET) is expressed as an appropriately scaled product of VPD (representing atmospheric aridity) and g_c (representing land-surface ability to supply water in response to atmospheric dryness). Although VPD is not explicitly used in the MEP model, its effect is included through specific humidity at the evaporating surface (i.e., q_s), and the increase of evaporative allocation at the continental scale is clearly related to the future increase in VPD (Figure S10b in Supporting Information S1). However, surface conductance g_c is projected to decrease in the future with larger decreases in SSP585 as compared to SSP245 (Figure S12 in Supporting Information S1), suggesting an increasing role of surface conditions constraining the ET flux. The lower surface conductance is likely to be caused by plant physiological responses to increasing CO_2 concentration, rising VPD (Grossiord et al., 2020), and drier soil (Figure S13 in Supporting Information S1), which would affect ESM simulations that provide the MEP inputs.

The projection results point to the need to better understand the relative contributions of future changes in R_n (increases of 7.8 W/m^2 for SSP245-END and 10 W/m^2 for SSP585-END, equivalent to 9.3% and 12% growth relative to the control period of 1961–1990), and evaporative allocation as well as the corresponding factors

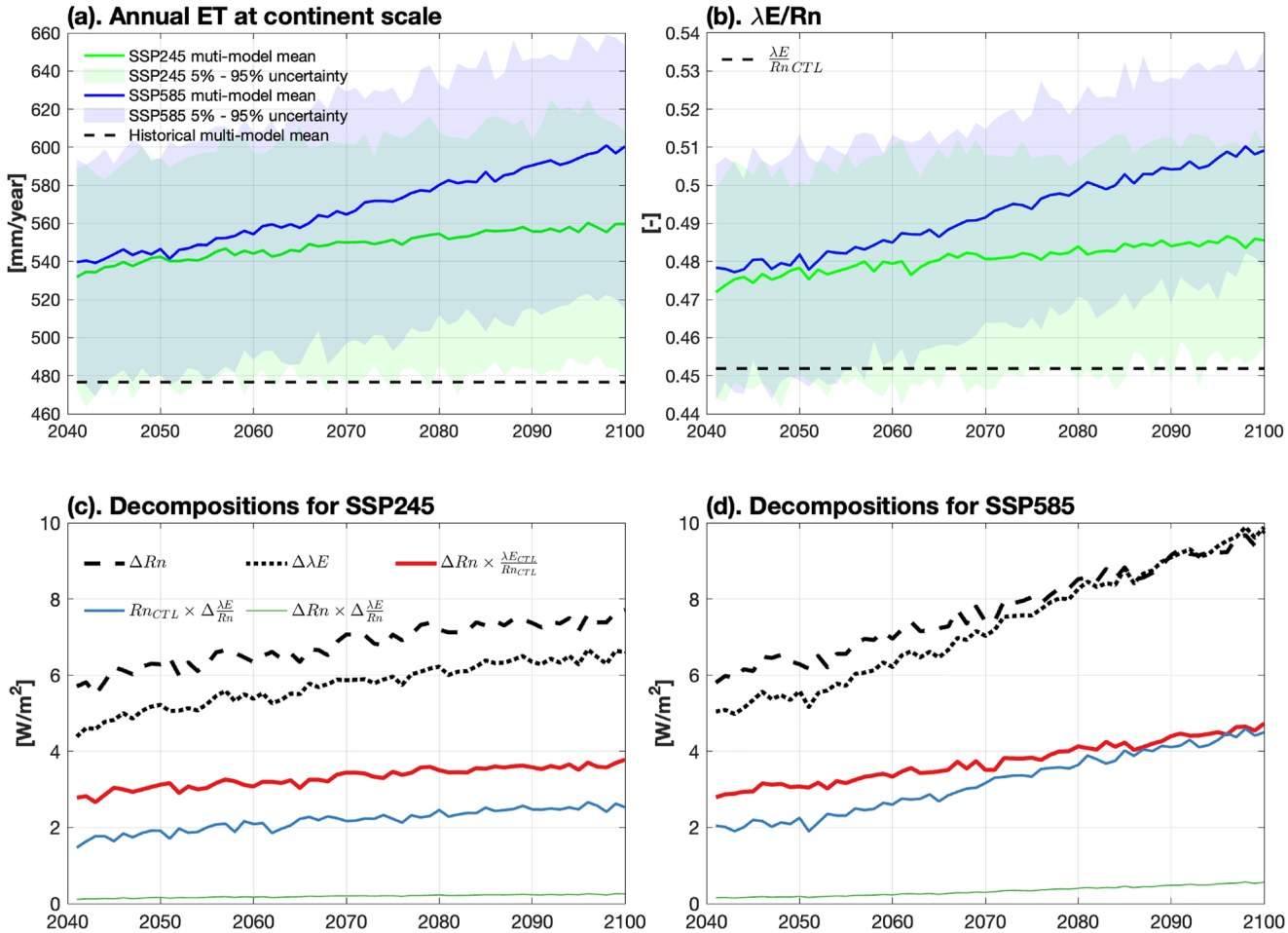

Figure 2. Time series of projected evapotranspiration, net radiation, and decomposition of ET changes into its contributing components averaged over CONUS for the SSP245 and SSP585 scenarios. (a) The projected time series of average annual ET and its 5%–95% uncertainty bounds based on the multi-model ensemble (equal weights were assigned to each model). (b) The time series of $^{\lambda E}/_{Rn}$ and the 5%–95% uncertainty bounds. Subplots (c) and (d) show the times series of changes in net radiation (ΔRn) and latent heat flux ($\Delta\lambda E$), as well as the decomposition $\Delta\lambda E$ due to contributions from ΔRn and $\Delta^{\lambda E}/_{Rn}$ for SSP245 (subplot (c)) and SSP585 (subplot (d)) scenarios. The term $\Delta Rn \times {}^{\lambda E_{CTL}}/_{Rn_{CTL}}$ represents the change of λE caused by the change in Rn (red solid line), $Rn_{CTL} \times \Delta^{\lambda E}/_{Rn}$ represents the change of λE caused by the change in the $^{\lambda E}/_{Rn}$ fraction (blue solid line), and $\Delta Rn \times \Delta^{\lambda E}/_{Rn}$ is the interaction term (green solid line).

controlling land-surface conditions. Figure 2c suggests that in the SSP245 scenario ~58% of ET increase is attributable to increases in net radiative energy and this fraction remains nearly constant over the projection period of 2041–2100. In the SSP585 scenario, the relative contribution of changes in Rn decreases from 57% in the MID-century, to 47% by the END-century due to a noticeable increase in the evaporative allocation (Figure 2d). It is remarkable that by the end of the 21st century, the projected changes in ET become comparable and even greater than the enhancement of the near-surface net radiative energy (i.e., 2085–2100, Figure 2d).

It is crucial to understand the impacts of emission scenario on evaporative allocation to explain the growing importance of the changes in the partition of net radiative energy in the SSP585 scenario. We decompose the increase of ET caused by $^{\lambda E}/_{Rn}$ changes into the contributions from three factors: VPD, g_c, and Rn (Text S6 in Supporting Information S1). Specifically, VPD is projected to be higher (Figure S12 in Supporting Information S1), representing the most important factor driving the increase of evaporative allocation. Its impact has an increasing trend during the MID-century and remain nearly constant for the END-century (Figure 3a). VPD contribution to the dynamics of $^{\lambda E}/_{Rn}$ exhibits a greater variation in the SSP245 than in the SSP585 scenario. In a spatial context, this is especially evident over the "corn belt" region of the US Midwest, where the contribution of atmospheric aridity to the change in evaporative allocation is much smaller than in the other CONUS areas. Surface conductance is projected to decrease in warming climate (Figure S12 in Supporting Information S1),

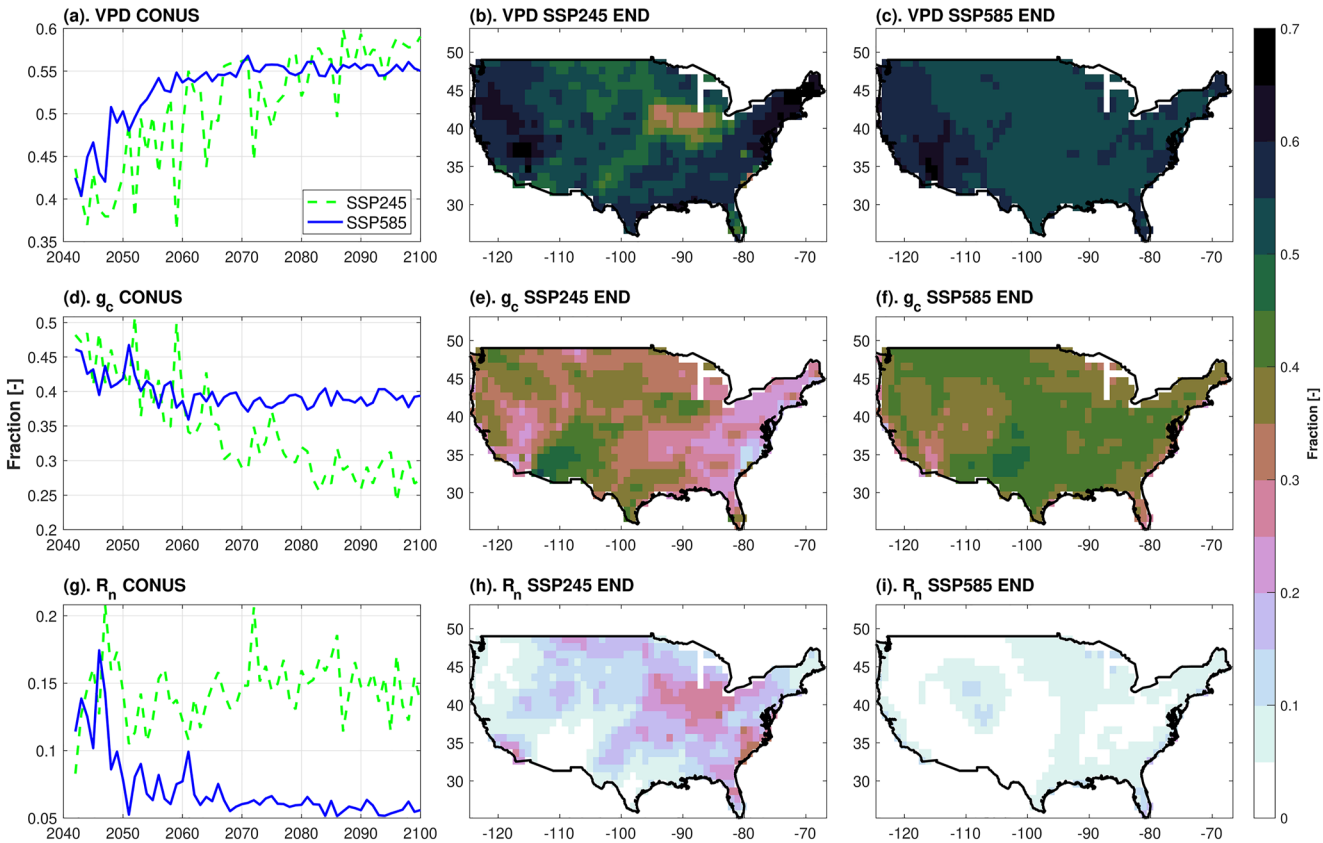

Figure 3. Relative fractions of (a)–(c) vapor pressure deficit (VPD), (d)–(f) surface conductance (g_c), and (g)–(i) net radiation (R_n) in the increase of $\frac{\lambda E}{R_n}$. The fractions are illustrated at the integrated CONUS scale (left plot panel), and as spatial distributions for the SSP245 scenario (middle panel) and the SSP585 scenario (right panel), for the 2071–2100 period.

thereby constraining the increase of evaporative allocation due to the enhanced VPD. Notably, while its spatial pattern delineates wetter eastern US as the area of weaker g_c control in the SSP245 scenario, it becomes substantially higher in the SSP585 scenario (Figures 3e and 3f). This alludes to a stronger land-surface control on ET changes in this emission scenario. Furthermore, in the "tug of war" between the ET flux-enhancing increase in VPD and flux-reducing decrease in g_c, both emission scenarios show the predominant role of VPD, indicating that $^{\lambda E}/_{\mathrm{Rn}}$ will predominantly grow due to the higher atmospheric demand, even though the land-surface will progressively impose higher resistance to ET flux. There may exist a threshold of temperature increase for g_c to be more dominant than VPD, since the increasing influence of VPD on the $^{\lambda E}/_{\mathrm{Rn}}$ change reaches its limit by the end of this century (Figure 3a).

R_n is another controlling factor in the projected increases of ET in both scenarios. While the overall increase of ET is predominantly caused by climate-induced rise in Rn (Figures 2c and 2d), its relative control on changes in $^{\lambda E}/_{\mathrm{Rn}}$ is weaker than that of VPD and g_s (Figures 3a, 3d and 3g). Furthermore, the contribution of Rn to the changes of $^{\lambda E}/_{\mathrm{Rn}}$ in SSP585 is negligible compared to that in SSP245 (Figures 3g–3i) during the late 21st century, which explains the higher control of g_c on evaporative allocation change in SSP585 (Figures 3d–3f). Our analysis also shows that surface conductance is the main factor constraining ET at higher projected temperatures, with a pronounced impact on ET increase due to the changes in $^{\lambda E}/_{\mathrm{Rn}}$ (Figure 2d).

3.3. Projections of Water Availability

Robust ET projections are further used to assess future water availability (Equation 2). Although the CONUS-averaged annual precipitation shows a significant increasing trend of 0.68 [mm/year/year] for the SSP245 scenario, it leads to a small, marginally significant positive trend in annual WA of 0.22 [mm/year/year] (Figures S14a and S14b in Supporting Information S1). The CONUS-averaged WA remains unchanged even for

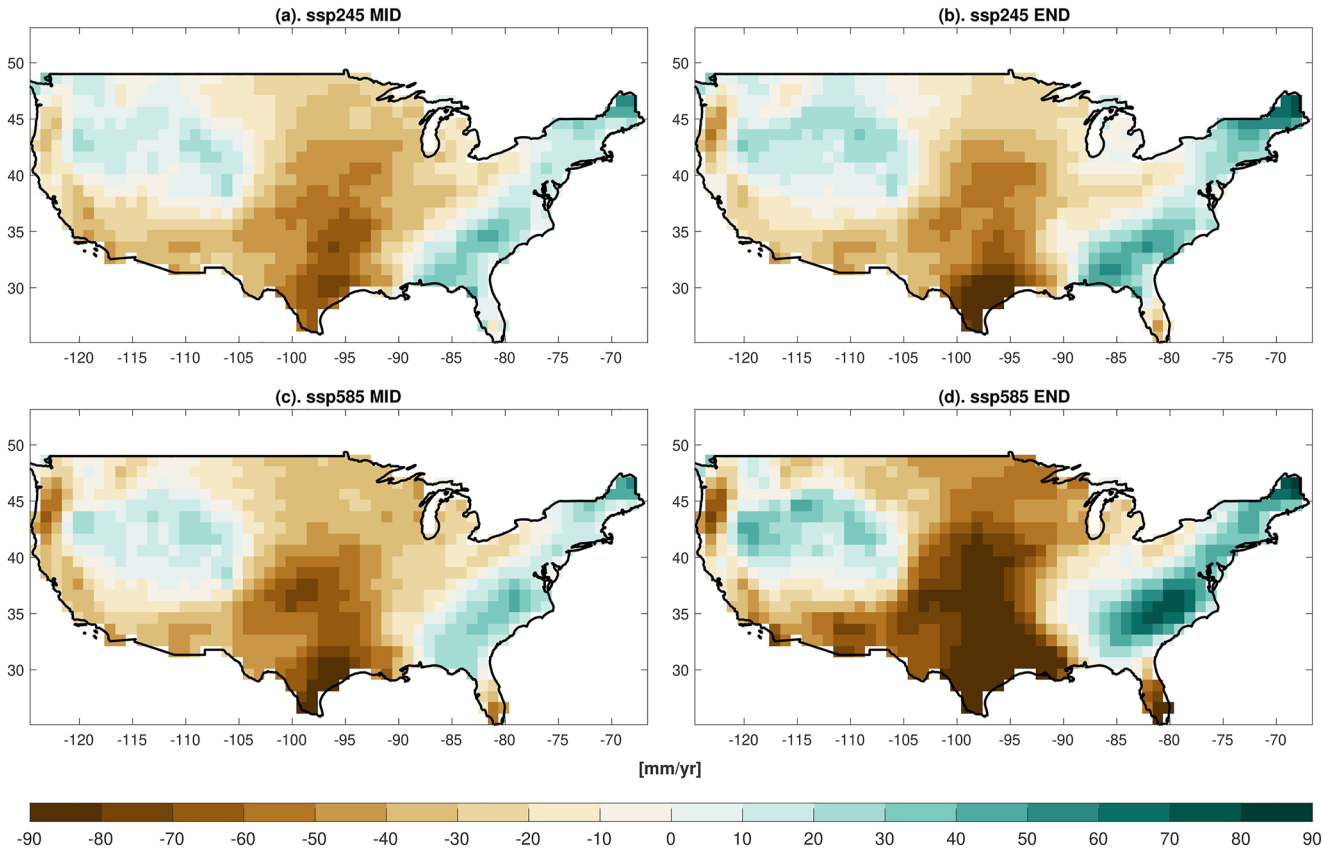

Figure 4. Change of annual water availability between the control (CTL) and future periods (FUT) using MEP-based ET projections. The difference (FUT–CTL) is estimated with the mean of equally weighted multi-model ensemble. "MID" represents the date difference with respect to 2041–2070 and 1961–1990 periods, and "END" represents the difference with respect to 2071–2100 and 1961–1990 periods. All of the results are shown at the 1° × 1° resolution.

a more significant trend of increasing precipitation under the SSP585 scenario (1.01 [mm/year/year]). The lack of temporal change in WA is arguably the direct result of the increased energy use by ET (i.e., the enhanced $^{\lambda E}/_{\mathrm{Rn}}$) implying that climate change intensifies flux exchange between the atmosphere and the land surface: increased precipitation tends to be returned to the atmosphere through the enhanced ET.

Although WA integrated over CONUS does not show a trend, WA exhibits a clear pattern of regional variability (Figure 4), with statistically significant projected increases in precipitation (Figure S15a and S15c in Supporting Information S1). Specifically, the spatial changes are similar for all scenarios and periods with increasing WA in the eastern coasts of the US (except Florida) and over the northern Rocky Mountain states, but a decrease of WA in the central and western US. Over the eastern US, where the ET projections are highly robust (RM > 0.8), the projected change of WA shows a slightly positive trend but statistically insignificant for both future scenarios (Figure S15b in Supporting Information S1). However, WA is projected to decrease significantly in the SSP585 scenario over the central and western US (Figure S15d in Supporting Information S1), although the robustness of the corresponding ET projection is not high. Furthermore, the spatial pattern of WA variability is more pronounced for the end of the century in the SSP585 scenario, suggesting that the higher projected temperature increase, the more uneven the distribution of surface water availability will be.

4. Discussion

This study is motivated by the lack of confident projections of ET despite its importance for understanding climate feedbacks and informing societal knowledge on future water resource distribution. The MEP model driven by outputs from the latest generation of ESMs improves ET estimation for the historical period and substantially increases the robustness of ET projections. The MEP model tends to underestimate the long-term mean annual ET by 6.8%. One possible reason for this underestimation is that evaporative loss from canopy

interception is not accounted for. Additionally, MEP model uses top soil moisture to represent water availability control on ET, but plants can take up water from a much larger soil reservoir (Agee et al., 2021; Brum et al., 2018; Li et al., 2021), especially during droughts. Another limitation of the MEP method is that the mass conservation is not explicitly considred, but MEP-based ET is nonetheless well constrained by precipitation (see Text S8 in Supporting Information S1). Furthermore, plant ecophysiological responses to transient climate are not explicitly accounted for in the MEP theory: but they are expected to be reflected in the coupled changes of all MEP model inputs and can be shown to lead to a qualitatively correct sensitivity of ET estimates (Text S9 in Supporting Information S1).

A nearly constant rate of increase of annual ET is projected when averaged at the CONUS scale: ~20 [mm/year] for every 1°C rise in near-surface air temperature. This ET growth is associated with the projected increases in land-surface net radiation and evaporative allocation of net available energy (that is, $^{\lambda E}/_{Rn}$. While the former factor generally dominates the ET increase in both considered CO_2 pathway scenarios, the contribution of the latter grows to nearly a half towards the end of the 21st century in the SSP585 scenario. In this scenario, the projected change in the ET energy flux even exceeds the total increase in land-surface net radiative energy.

This study finds that evaporative allocation grows in both CO_2 pathway scenarios. Contributions to this growth are dominated by the higher atmospheric aridity that drives the conversion of liquid water to vapor under the global warming. Concurrently, the surface conductance to vapor flux is projected to decrease, counteracting the effect of increasing VPD (i.e., the "tug of war" analogy). The growth of evaporative allocation and ET implies that the reduction in surface conductance cannot fully offset the atmospheric demand for water vapor. Further, the more significant increase of evaporative allocation in the SSP585 scenario is also associated with the greater influence of land-surface controls on ET flux. This is because the Clausius-Clapeyron relationship (Brutsaert, 2005) dictates a greater rate of VPD increase at higher temperatures in the SSP585 pathway, and if the surface conditions cannot keep up with the atmospheric water demand, they exert stronger control on the flux. The relative roles of demand versus supply controls will determine the distribution of future ET over the CONUS, and our results demonstrate clear regional distributions related to a given emission scenario. The attribution of surface conductance however includes uncertainties because surface soil moisture can overestimate water stress and physiology impacts are not explicitly included. However, an attribution analysis conducted with the ESM-based ET ensemble leads to similar conclusions showing only a slightly higer control from surface conductance (not shown).

The increase of ET nearly balances the projected increase of precipitation in the future. While there is a weak increase of water availability in the SSP245 scenario, no significant changes in water availability at the CONUS scale are projected for the SSP585 pathway. However, the change of water availability shows pronounced regional variability, with different areas projected to have a decline (central and western US), while others an increase (eastern coasts of the US) in the mean long-term WA. These projected changes imply greater challenges for water management in a warming climate, especially under the high emission scenario: the results show the largest increase of spatial variability in the projected water availability due to the increase of evaporative allocation and ET. As this research confirms, one of the detrimental consequences of global warming is the proliferation of non-equitable distribution of water availability (Rogelj et al., 2012).

Data Availability Statement

The CIMP6 climate model projections that list in Table S1 in Supporting Information S1 were downloaded from https://esgf-node.llnl.gov/projects/cmip6/. We used the MODIS NDVI (MOD13C2), which can be downloaded from http://doi.org/10.5067/MODIS/MOD13C2.006. The long-term gridded precipitation and runoff for the water budget method can be retrieved from https://psl.noaa.gov/data/gridded/data.livneh.html. The observed precipitation data were downloaded from WebMET Samson Surface Met Data (http://www.webmet.com/met_data.html). The observed streamflow was obtained from all the available USGS (https://www.usgs.gov) streamflow gauges with measurements of more than 15 years during 1961–1990, and the gauge information and downloading script can be found at https://doi.org/10.5281/zenodo.7741957. The MEP code and scripts used in this study to process the data and plot the results can be found at https://doi.org/10.5281/zenodo.6568460.

Acknowledgments
V.I. acknowledges the support of awards NSF DEB 1754163 and 2111028, NSF ICER 2126792, NSF OPP 1725654, and the gift from the Google Inc. that "seeded" this research. J.W. is sponsored by NSF OPP-1724633 and NNA2126797. Partial support of J.W.'s research is provided by NASA SMAP program. E.A. was supported by the NASA Earth and Space Science Fellowship (17-EARTH17F-84) and in part by the Next Generation Ecosystem Experiments-Tropics, funded by the U.S. Department of Energy, Office of Science, Office of Biological and Environmental Research. ORNL is managed by UT-Battelle, LLC, for the DOE contract DE-AC05-100800OR22725. We thank Dr. T. Taylor for helping with the abstract during the manuscript preparation.

References

Agee, E., He, L., Bisht, G., Couvreur, V., Shahbaz, P., Meunier, F., et al. (2021). Root lateral interactions drive water uptake patterns under water limitation. *Advances in Water Resources*, *151*, 103896. https://doi.org/10.1016/j.advwatres.2021.103896

Ajjur, S. B., & Al-Ghamdi, S. G. (2021). Evapotranspiration and water availability response to climate change in the Middle East and North Africa. *Climatic Change*, *166*(3), 28. https://doi.org/10.1007/s10584-021-03122-z

Berg, A., & Sheffield, J. (2019). Evapotranspiration partitioning in CMIP5 models: Uncertainties and future projections. *Journal of Climate*, *32*(10), 2653–2671. https://doi.org/10.1175/jcli-d-18-0583.1

Brum, M., Vadeboncoeur, M. A., Ivanov, V., Asbjornsen, H., Saleska, S., Alves, L. F., et al. (2018). Hydrological niche segregation defines forest structure and drought tolerance strategies in a seasonal Amazon forest. *Journal of Ecology*, *0*(0), 318–333. https://doi.org/10.1111/1365-2745.13022

Brutsaert, W. (2005). *Hydrology: An introduction*. Cambridge university press.

Dai, A. (2013). Increasing drought under global warming in observations and models. *Nature Climate Change*, *3*(1), 52–58. https://doi.org/10.1038/nclimate1633

Eyring, V., Bony, S., Meehl, G. A., Senior, C. A., Stevens, B., Stouffer, R. J., & Taylor, K. E. (2016). Overview of the coupled model intercomparison project Phase 6 (CMIP6) experimental design and organization. *Geoscientific Model Development*, *9*(5), 1937–1958. https://doi.org/10.5194/gmd-9-1937-2016

Fisher, J. B., Melton, F., Middleton, E., Hain, C., Anderson, M., Allen, R., et al. (2017). The future of evapotranspiration: Global requirements for ecosystem functioning, carbon and climate feedbacks, agricultural management, and water resources. *Water Resources Research*, *53*(4), 2618–2626. https://doi.org/10.1002/2016wr020175

Good, S. P., Noone, D., & Bowen, G. (2015). Hydrologic connectivity constrains partitioning of global terrestrial water fluxes. *Science*, *349*(6244), 175–177. https://doi.org/10.1126/science.aaa5931

Grossiord, C., Buckley, T. N., Cernusak, L. A., Novick, K. A., Poulter, B., Siegwolf, R. T., et al. (2020). Plant responses to rising vapor pressure deficit. *New Phytologist*, *226*(6), 1550–1566. https://doi.org/10.1111/nph.16485

Hajji, I., Nadeau, D. F., Music, B., Anctil, F., & Wang, J. F. (2018). Application of the maximum entropy production model of evapotranspiration over partially vegetated water-limited land surfaces. *Journal of Hydrometeorology*, *19*(6), 989–1005. https://doi.org/10.1175/jhm-d-17-0133.1

Huang, S.-Y., Deng, Y., & Wang, J. (2017). Revisiting the global surface energy budgets with maximum-entropy-production model of surface heat fluxes. *Climate Dynamics*, *49*(5), 1531–1545. https://doi.org/10.1007/s00382-016-3395-x

Humphrey, V., Berg, A., Ciais, P., Gentine, P., Jung, M., Reichstein, M., et al. (2021). Soil moisture–atmosphere feedback dominates land carbon uptake variability. *Nature*, *592*(7852), 65–69. https://doi.org/10.1038/s41586-021-03325-5

Isabelle, P. E., Viens, L., Nadeau, D. F., Anctil, F., Wang, J., & Maheu, A. (2021). Sensitivity analysis of the maximum entropy production method to model evaporation in boreal and temperate forests. *Geophysical Research Letters*, *48*(13), e2020GL091919. https://doi.org/10.1029/2020gl091919

Jung, M., Reichstein, M., Ciais, P., Seneviratne, S. I., Sheffield, J., Goulden, M. L., et al. (2010). Recent decline in the global land evapotranspiration trend due to limited moisture supply. *Nature*, *467*(7318), 951–954. https://doi.org/10.1038/nature09396

Knutti, R., & Sedláček, J. (2012). Robustness and uncertainties in the new CMIP5 climate model projections. *Nature Climate Change*, *3*(4), 369–373. https://doi.org/10.1038/nclimate1716

Konapala, G., & Mishra, A. (2020). Quantifying climate and catchment control on hydrological drought in the continental United States. *Water Resources Research*, *56*(1), e2018WR024620. https://doi.org/10.1029/2018wr024620

Lemordant, L., Gentine, P., Swann, A. S., Cook, B. I., & Scheff, J. (2018). Critical impact of vegetation physiology on the continental hydrologic cycle in response to increasing CO_2. *Proceedings of the National Academy of Sciences*, *115*(16), 4093–4098. https://doi.org/10.1073/pnas.1720712115

Li, L., Yang, Z.-L., Matheny, A. M., Zheng, H., Swenson, S. C., Lawrence, D. M., et al. (2021). Representation of plant hydraulics in the Noah-MP land surface Model: Model development and multi-scale evaluation. *Journal of Advances in Modeling Earth Systems*, *13*(4), e2020MS002214. https://doi.org/10.1029/2020ms002214

Liu, L., Gudmundsson, L., Hauser, M., Qin, D., Li, S., & Seneviratne, S. I. (2020). Soil moisture dominates dryness stress on ecosystem production globally. *Nature Communications*, *11*(1), 4892. https://doi.org/10.1038/s41467-020-18631-1

Livneh, B., Rosenberg, E. A., Lin, C., Nijssen, B., Mishra, V., Andreadis, K. M., et al. (2013). A long-term hydrologically based dataset of land surface fluxes and states for the conterminous United States: Update and extensions. *Journal of Climate*, *26*(23), 9384–9392. https://doi.org/10.1175/jcli-d-12-00508.1

Lu, J., Wang, G., Li, S., Feng, A., Zhan, M., Jiang, T., et al. (2021). Projected land evaporation and its response to vegetation greening over China under multiple scenarios in the CMIP6 models. *Journal of Geophysical Research: Biogeosciences*, *126*(9), e2021JG006327. https://doi.org/10.1029/2021jg006327

Mao, J., Fu, W., Shi, X., Ricciuto, D. M., Fisher, J. B., Dickinson, R. E., et al. (2015). Disentangling climatic and anthropogenic controls on global terrestrial evapotranspiration trends. *Environmental Research Letters*, *10*(9), 094008. https://doi.org/10.1088/1748-9326/10/9/094008

Milly, P. C. D., & Dunne, K. A. (2016). Potential evapotranspiration and continental drying. *Nature Climate Change*, *6*(10), 946–949. https://doi.org/10.1038/nclimate3046

Miralles, D. G., van den Berg, M. J., Gash, J. H., Parinussa, R. M., de Jeu, R. A. M., Beck, H. E., et al. (2014). El Niño–La Niña cycle and recent trends in continental evaporation. *Nature Climate Change*, *4*(2), 122–126. https://doi.org/10.1038/nclimate2068

Nearing, G. S., Moran, M. S., Scott, R. L., & Ponce-Campos, G. (2012). Coupling diffusion and maximum entropy models to estimate thermal inertia. *Remote Sensing of Environment*, *119*, 222–231. https://doi.org/10.1016/j.rse.2011.12.012

Novick, K. A., Ficklin, D. L., Stoy, P. C., Williams, C. A., Bohrer, G., Oishi, A., et al. (2016). The increasing importance of atmospheric demand for ecosystem water and carbon fluxes. *Nature Climate Change*, *6*(11), 1023–1027. https://doi.org/10.1038/nclimate3114

Oki, T., & Kanae, S. (2006). Global hydrological cycles and world water resources. *Science*, *313*(5790), 1068–1072. https://doi.org/10.1126/science.1128845

O'Neill, B. C., Kriegler, E., Ebi, K. L., Kemp-Benedict, E., Riahi, K., Rothman, D. S., et al. (2017). The roads ahead: Narratives for shared socioeconomic pathways describing world futures in the 21st century. *Global Environmental Change*, *42*, 169–180. https://doi.org/10.1016/j.gloenvcha.2015.01.004

Oren, R., Sperry, J. S., Katul, G. G., Pataki, D. E., Ewers, B. E., Phillips, N., & Schäfer, K. V. R. (1999). Survey and synthesis of intra- and interspecific variation in stomatal sensitivity to vapour pressure deficit. *Plant, Cell and Environment*, *22*(12), 1515–1526. https://doi.org/10.1046/j.1365-3040.1999.00513.x

Rogelj, J., Meinshausen, M., & Knutti, R. (2012). Global warming under old an new scenarios using IPCC climate sensitivity range estimates. *Nature Climate Change*, *2*(4), 248–253. https://doi.org/10.1038/nclimate1385

Sellers, P., Dickinson, R., Randall, D., Betts, A., Hall, F., Berry, J., et al. (1997). Modeling the exchanges of energy, water, and carbon between continents and the atmosphere. *Science*, *275*(5299), 502–509. https://doi.org/10.1126/science.275.5299.502

Seneviratne, S. I., Corti, T., Davin, E. L., Hirschi, M., Jaeger, E. B., Lehner, I., et al. (2010). Investigating soil moisture–climate interactions in a changing climate: A review. *Earth-Science Reviews*, *99*(3), 125–161. https://doi.org/10.1016/j.earscirev.2010.02.004

Shanafield, M., Cook, P. G., Gutierrez-Jurado, H. A., Faux, R., Cleverly, J., & Eamus, D. (2015). Field comparison of methods for estimating groundwater discharge by evaporation and evapotranspiration in an arid-zone playa. *Journal of Hydrology*, *527*, 1073–1083. https://doi.org/10.1016/j.jhydrol.2015.06.003

Sullivan, R. C., Kotamarthi, V. R., & Feng, Y. (2019). Recovering evapotranspiration trends from biased CMIP5 simulations and sensitivity to changing climate over North America. *Journal of Hydrometeorology*, *20*(8), 1619–1633. https://doi.org/10.1175/jhm-d-18-0259.1

Sulman, B. N., Roman, D. T., Yi, K., Wang, L., Phillips, R. P., & Novick, K. A. (2016). High atmospheric demand for water can limit forest carbon uptake and transpiration as severely as dry soil. *Geophysical Research Letters*, *43*(18), 9686–9695. https://doi.org/10.1002/2016gl069416

Sun, H., Chen, J., Yang, Y., Yan, D., Xue, J., Wang, J., & Zhang, W. (2022). Assessment of long-term water stress for ecosystems across China using the maximum entropy production theory-based evapotranspiration product. *Journal of Cleaner Production*, *349*, 131414. https://doi.org/10.1016/j.jclepro.2022.131414

Swann, A. L. S., Hoffman, F. M., Koven, C. D., & Randerson, J. T. (2016). Plant responses to increasing CO2 reduce estimates of climate impacts on drought severity. *Proceedings of the National Academy of Sciences*, *113*(36), 10019–10024. https://doi.org/10.1073/pnas.1604581113

Tor-ngern, P., Oren, R., Ward, E. J., Palmroth, S., McCarthy, H. R., & Domec, J.-C. (2015). Increases in atmospheric CO2 have little influence on transpiration of a temperate forest canopy. *New Phytologist*, *205*(2), 518–525. https://doi.org/10.1111/nph.13148

Trenberth, K. E., Fasullo, J. T., & Kiehl, J. (2009). Earth's global energy budget. *Bulletin of the American Meteorological Society*, *90*(3), 311–323. https://doi.org/10.1175/2008bams2634.1

Wang, J. F., & Bras, R. L. (2009). A model of surface heat fluxes based on the theory of maximum entropy production. *Water Resources Research*, *45*(11), W11422. https://doi.org/10.1029/2009wr007900

Wang, J. F., & Bras, R. L. (2011). A model of evapotranspiration based on the theory of maximum entropy production. *Water Resources Research*, *47*(3), W03521. https://doi.org/10.1029/2010wr009392

Wang, J. F., Bras, R. L., Nieves, V., & Deng, Y. (2014). A model of energy budgets over water, snow, and ice surfaces. *J Geophys Res-Atmos*, *119*(10), 6034–6051. https://doi.org/10.1002/2013jd021150

Wei, T., Yang, S., Moore, J. C., Shi, P., Cui, X., Duan, Q., et al. (2012). Developed and developing world responsibilities for historical climate change and CO_2 mitigation. *Proceedings of the National Academy of Sciences of the United States of America*, *109*(32), 12911–12915. https://doi.org/10.1073/pnas.1203282109

Wild, M., Grieser, J., & Schär, C. (2008). Combined surface solar brightening and increasing greenhouse effect support recent intensification of the global land-based hydrological cycle. *Geophysical Research Letters*, *35*(17), L17706. https://doi.org/10.1029/2008gl034842

Xiao, M., Yu, Z., Kong, D., Gu, X., Mammarella, I., Montagnani, L., et al. (2020). Stomatal response to decreased relative humidity constrains the acceleration of terrestrial evapotranspiration. *Environmental Research Letters*, *15*(9), 094066. https://doi.org/10.1088/1748-9326/ab9967

Xu, D., Agee, E., Wang, J., & Ivanov, V. Y. (2019). Estimation of evapotranspiration of Amazon rainforest using the maximum entropy production method. *Geophysical Research Letters*, *0*(0), 1402–1412. https://doi.org/10.1029/2018gl080907

Yao, Y., Liang, S., Li, X., Liu, S., Chen, J., Zhang, X., et al. (2016). Assessment and simulation of global terrestrial latent heat flux by synthesis of CMIP5 climate models and surface eddy covariance observations. *Agricultural and Forest Meteorology*, *223*, 151–167. https://doi.org/10.1016/j.agrformet.2016.03.016

Yuan, W., Zheng, Y., Piao, S., Ciais, P., Lombardozzi, D., Wang, Y., et al. (2019). Increased atmospheric vapor pressure deficit reduces global vegetation growth. *Science Advances*, *5*(8), eaax1396. https://doi.org/10.1126/sciadv.aax1396

Zeng, Z., Piao, S., Lin, X., Yin, G., Peng, S., Ciais, P., & Myneni, R. B. (2012). Global evapotranspiration over the past three decades: Estimation based on the water balance equation combined with empirical models. *Environmental Research Letters*, *7*(1), 014026. https://doi.org/10.1088/1748-9326/7/1/014026

Zhang, K., Kimball, J. S., Nemani, R. R., Running, S. W., Hong, Y., Gourley, J. J., & Yu, Z. (2015). Vegetation greening and climate change promote multidecadal rises of global land evapotranspiration. *Scientific Reports*, *5*(1), 15956. https://doi.org/10.1038/srep15956

Zhang, Y., Peña-Arancibia, J. L., McVicar, T. R., Chiew, F. H. S., Vaze, J., Liu, C., et al. (2016). Multi-decadal trends in global terrestrial evapotranspiration and its components. *Scientific Reports*, *6*(1), 19124. https://doi.org/10.1038/srep19124

Zhu, Z., Piao, S., Myneni, R. B., Huang, M., Zeng, Z., Canadell, J. G., et al. (2016). Greening of the Earth and its drivers. *Nature Climate Change*, *6*(8), 791–795. https://doi.org/10.1038/nclimate3004

References From the Supporting Information

Ban-Weiss, G. A., Bala, G., Cao, L., Pongratz, J., & Caldeira, K. (2011). Climate forcing and response to idealized changes in surface latent and sensible heat. *Environmental Research Letters*, *6*(3), 034032. https://doi.org/10.1088/1748-9326/6/3/034032

Carlson, T. N., & Ripley, D. A. (1997). On the relation between NDVI, fractional vegetation cover, and leaf area index. *Remote Sensing of Environment*, *62*(3), 241–252. https://doi.org/10.1016/s0034-4257(97)00104-1

Cui, Z., Wang, Y., Zhang, G. J., Yang, M., Liu, J., & Wei, L. (2022). Effects of improved simulation of precipitation on evapotranspiration and its partitioning over land. *Geophysical Research Letters*, *49*(5), e2021GL097353. https://doi.org/10.1029/2021gl097353

Didan, K. (2015). MOD13C2 MODIS/terra vegetation indices monthly L3 global 0.05 Deg CMG V006 [Dataset]. NASA EOSDIS Land Processes DAAC. https://doi.org/10.5067/MODIS/MOD13C2.006

Ellison, D., Morris, C. E., Locatelli, B., Sheil, D., Cohen, J., Murdiyarso, D., et al. (2017). Trees, forests and water: Cool insights for a hot world. *Global Environmental Change*, *43*, 51–61. https://doi.org/10.1016/j.gloenvcha.2017.01.002

Farouki, O. (1982). *Thermal properties of soils*. Rep. CRREL Monogr No. 81-1. U.S. Army Cold Regions Research and Engineering Laboratory.

Fowler, H. J., Blenkinsop, S., & Tebaldi, C. (2007). Linking climate change modelling to impacts studies: Recent advances in downscaling techniques for hydrological modelling. *International Journal of Climatology*, *27*(12), 1547–1578. https://doi.org/10.1002/joc.1556

Hall, A., & Manabe, S. (1999). The role of water vapor feedback in unperturbed climate variability and global warming. *Journal of Climate*, *12*(8), 2327–2346. https://doi.org/10.1175/1520-0442(1999)012<2327:trowvf>2.0.co;2

Ivanov, V. Y., Bras, R. L., & Vivoni, E. R. (2008). Vegetation-hydrology dynamics in complex terrain of semiarid areas: 1. A mechanistic approach to modeling dynamic feedbacks. *Water Resources Research*, *44*(3), W03429. https://doi.org/10.1029/2006wr005588

Kim, J., Ivanov, V. Y., & Fatichi, S. (2015). *Climate change and uncertainty assessment over a hydroclimatic transect of Michigan*. Stochastic Environmental Research and Risk Assessment.

Knutti, R., Furrer, R., Tebaldi, C., Cermak, J., & Meehl, G. A. (2010). Challenges in combining projections from multiple climate models. *Journal of Climate*, *23*(10), 2739–2758. https://doi.org/10.1175/2009jcli3361.1

Lawrence, D. M., Fisher, R. A., Koven, C. D., Oleson, K. W., Swenson, S. C., Bonan, G., et al. (2019). The community land model version 5: Description of new features, benchmarking, and impact of forcing uncertainty. *Journal of Advances in Modeling Earth Systems*, *11*(12), 4245–4287. https://doi.org/10.1029/2018ms001583

Mearns, L. O., Sain, S., Leung, L. R., Bukovsky, M. S., McGinnis, S., Biner, S., et al. (2013). Climate change projections of the North American regional climate change assessment program (NARCCAP). *Climatic Change*, *120*(4), 965–975. https://doi.org/10.1007/s10584-013-0831-3

Mueller, B., & Seneviratne, S. I. (2014). Systematic land climate and evapotranspiration biases in CMIP5 simulations. *Geophysical Research Letters*, *41*(1), 128–134. https://doi.org/10.1002/2013gl058055

Mueller, B., Seneviratne, S. I., Jimenez, C., Corti, T., Hirschi, M., Balsamo, G., et al. (2011). Evaluation of global observations-based evapotranspiration datasets and IPCC AR4 simulations. *Geophysical Research Letters*, *38*(6), L06402. https://doi.org/10.1029/2010gl046230

Mueller, B., Hirschi, M., Jimenez, C., Ciais, P., Dirmeyer, P. A., Dolman, A. J., et al. (2013). Benchmark products for land evapotranspiration: LandFlux-EVAL multi-data set synthesis. *Hydrology and Earth System Sciences*, *17*(10), 3707–3720. https://doi.org/10.5194/hess-17-3707-2013

Oleson, K., Lawrence, D. M., Bonan, G. B., Drewniak, B., Huang, M., Koven, C. D., et al. (2013). Technical description of version 4.5 of the community land model (CLM) (No. NCAR/TN-503+STR). https://doi.org/10.5065/D6RR1W7M

Pettorelli, N. (2013). *The normalized difference vegetation index* (pp. 1–208). The Normalized Difference Vegetation Index.

Schwalm, C. R., Huntinzger, D. N., Michalak, A. M., Fisher, J. B., Kimball, J. S., Mueller, B., et al. (2013). Sensitivity of inferred climate model skill to evaluation decisions: A case study using CMIP5 evapotranspiration. *Environmental Research Letters*, *8*(2), 024028. https://doi.org/10.1088/1748-9326/8/2/024028

Sen, P. K. (1968). Estimates of the regression coefficient based on Kendall's Tau. *Journal of the American Statistical Association*, *63*(324), 1379–1389. https://doi.org/10.1080/01621459.1968.10480934

Seo, K.-W., Waliser, D. E., Tian, B., Famiglietti, J. S., & Syed, T. H. (2009). Evaluation of global land-to-ocean fresh water discharge and evapotranspiration using space-based observations. *Journal of Hydrology*, *373*(3), 508–515. https://doi.org/10.1016/j.jhydrol.2009.05.014

Smith, R. L., Tebaldi, C., Nychka, D., & Mearns, L. O. (2009). Bayesian modeling of uncertainty in ensembles of climate models. *Journal of the American Statistical Association*, *104*(485), 97–116. https://doi.org/10.1198/jasa.2009.0007

Stoy, P. C., Roh, J., & Bromley, G. T. (2022). It's the heat and the humidity: The complementary roles of temperature and specific humidity to recent changes in the energy content of the near-surface atmosphere. *Geophysical Research Letters*, *49*(4), e2021GL096628. https://doi.org/10.1029/2021gl096628

van Heerwaarden, C. C., Vilà-Guerau de Arellano, J., & Teuling, A. J. (2010). Land-atmosphere coupling explains the link between pan evaporation and actual evapotranspiration trends in a changing climate. *Geophysical Research Letters*, *37*(21), L21401. https://doi.org/10.1029/2010gl045374

Wang, Z., Zhan, C., Ning, L., & Guo, H. (2021). Evaluation of global terrestrial evapotranspiration in CMIP6 models. *Theoretical and Applied Climatology*, *143*(1), 521–531. https://doi.org/10.1007/s00704-020-03437-4

Wilson, K., Goldstein, A., Falge, E., Aubinet, M., Baldocchi, D., Berbigier, P., et al. (2002). Energy balance closure at FLUXNET sites. *Agricultural and Forest Meteorology*, *113*(1–4), 223–243. https://doi.org/10.1016/s0168-1923(02)00109-0

Xu, D., Ivanov, V. Y., Kim, J., & Fatichi, S. (2018). *On the use of observations in assessment of multi-model climate ensemble*. Stochastic Environmental Research and Risk Assessment.